# Effects of parton intrinsic transverse momentum on photon production in hard-scattering processes

Cheuk-Yin Wong
*Physics Division, Oak Ridge National Laboratory, Oak Ridge, Tennessee 37831*

Hui Wang
*Physics Division, Oak Ridge National Laboratory, Oak Ridge, Tennessee 37831*
*and China Institute of Atomic Energy, Beijing, China*

(Received 20 February 1998)

We calculate the photon production cross section arising from the hard scattering of partons in nucleon-nucleon collisions by taking into account the intrinsic parton transverse momentum distribution and the next-to-leading-order contributions. As first pointed out by Owens, the inclusion of the intrinsic transverse momentum distribution of partons leads to an enhancement of photon production cross section in the region of photon transverse momenta of a few GeV/$c$ for nucleon-nucleon collisions at a center-of-mass energy of a few tens of GeV. The enhancement increases as $\sqrt{s}$ decreases. Such an enhancement is an important consideration in the region of photon momenta under investigation in high-energy heavy-ion collisions. [S0556-2813(98)04007-2]

PACS number(s): 25.75.−q, 24.85.+p, 13.85.Qk, 13.75.Cs

## I. INTRODUCTION

Currently, high-energy heavy-ion collisions are used to produce matter under extreme conditions. One of the objectives is to search for the quark-gluon plasma (QGP) which is expected to exist at high temperatures and/or high baryon densities. (For an introduction to this field, see Refs. [1–5].) Photons arising from the electromagnetic interactions of the constituents of the plasma will provide information on the properties of the plasma at the time of their production. Since photons are hardly absorbed by the produced medium, they form a relatively ''clean'' probe to study the state of the quark-gluon plasma. The detection of these photons during the quark-gluon plasma phase will be of great interest in probing the state of the quark-gluon plasma, if it is ever produced [6–15].

Photons are also produced by many other processes in heavy-ion reactions. They can originate from the decay of $\pi^0$ and $\eta^0$. As $\pi^0$ particles are copiously produced in strong interactions between nucleons, photons originating from the decay of $\pi^0$ are much more abundant than photons produced by electromagnetic interactions of the constituents of the quark-gluon plasma. The photons from the decay of $\pi^0$ and $\eta^0$ can be subtracted out by making a direct measurement of their yield, obtained by combining pairs of photons. Because of the large number of $\pi^0$ produced, this subtraction is a laborious task, but much progress has been made to provide meaningful results after the subtraction of the photons from the $\pi^0$ and $\eta^0$ backgrounds [11–13]. Photon measurements obtained after the subtraction of the photons from meson decays are conveniently called measurements of ''direct photons.''

Direct photons are produced from the interaction of matter in the QGP phase, a mixed QGP and hadron phase, a pure hadron gas, and hard QCD processes [4,5]. Different processes give rise to photons in different momentum regions. We are interested in photons from the quark-gluon plasma which are found predominantly in the region of photons with low transverse momentum, extending to the region of intermediate transverse momentum of 1–3 GeV/$c$. At photon energies up to 2 GeV, photons can come from the decay of $\pi^0$ and $\eta^0$ resonances as well as from $\rho, \omega, \eta'$, and $a_1$, and the interaction of the hadron matter via $\pi\rho \to \gamma\rho$ and $\pi\pi \to \gamma\pi$ reactions (see for example Refs. [14–17]). One may wish to go to the region of photon transverse momentum $p_{\gamma T} > 2$ GeV/$c$. If a hot quark-gluon plasma is formed initially, clear signals of photons from the plasma could be visible by examining photons with $p_{\gamma T}$ in the range 2–3 GeV/$c$ [8–10]. On the other hand, photons in this region of transverse momenta are also produced by the collision of partons of the projectile nucleons with partons of the target nucleons. Such a contribution must be subtracted in order to infer the net photons from the quark-gluon plasma sources.

Recent investigations on photon production by parton collisions in hadron-hadron collisions include the work by Aurenche, Baier, Douiri, Fontannaz, and Schiff [18,19] and by Baer, Ohnemus, and Owens [20], who have performed QCD calculations up to second order in $\alpha$. Extensive comparisons with experimental data have been carried out covering a large range of incident energies and photon transverse momenta. In these QCD calculations, as well as other similar QCD calculations [21], the intrinsic transverse momenta of the partons have been neglected.

Because of the finite size of the transverse dimension of a nucleon, one expects that the partons in a nucleon have an intrinsic transverse momentum distribution with a width of the order of $\sqrt{2}\hbar/0.5$ fm. Soft gluon radiation also contributes to the parton intrinsic transverse momentum. The intrinsic transverse momentum distribution affects the distribution of the produced photons. Previous investigations of the photon transverse momentum distribution in leading-order (LO) calculations with a constant $K$-factor already indicate the importance of the intrinsic transverse momentum of the partons [22]. For $p_{\gamma T}$ from 3 to 8 GeV/$c$, the photon production

 

cross sections for hadron-hadron collisions at 19.4 GeV $<\sqrt{s}<63$ GeV are enhanced when the intrinsic transverse momentum distribution is taken into account, in agreement with earlier measurements. These findings are further supported by recent experimental and theoretical investigations for hadron-proton collisions at $\sqrt{s}=31.7$ and 38.8 GeV [23]. The enhancement increases as $\sqrt{s}$ decreases. Therefore, in the region of our interest involving photons with $p_{\gamma T}$ of about 2–3 GeV/$c$ at a center-of-mass energy of about 20 GeV, as in the measurements of the WA80 and the WA98 Collaborations [11,12], the intrinsic transverse momentum of partons plays an important role and cannot be neglected. How the photon transverse momentum distributions at different $\sqrt{s}$ are affected by the parton intrinsic transverse momentum is the main subject of our investigation.

There is also another important effect which is important in photon production. Previous calculations of photon production indicate the importance of higher-order QCD terms [18–20]. The next-to-leading-order calculations lead to a correction factor, the $K$-factor, with a magnitude of about 2. It is necessary to include the effects of the next-to-leading-order corrections. One expects that the next-to-leading-order effects are nearly independent of the intrinsic transverse momentum. One can include the effects of the intrinsic transverse momentum and the next-to-leading-order corrections by first treating them separately and then combining them as independent multiplicative factors. The final results can be compared with experimental data. Good agreement with experimental data at different reaction energies will form the basis of extrapolation to the region of interest in high-energy heavy-ion collisions.

Previous work by Cleymans *et al.* [21] on photon production in $pp$ collisions covers a region from $\sqrt{s}=23$ GeV to 1.8 TeV. These authors use the next-to-leading-order calculation program of Aurenche *et al.* [18], without assuming parton intrinsic transverse momentum. However, the results of these authors cannot be interpreted as the conclusive evidence for the absence of any parton intrinsic momentum effect at energies of $\sqrt{s}\sim 20$ GeV, because their theoretical results are lower than the UA6 data at $\sqrt{s}=24.3$ GeV by about a factor of 2 (see Fig. 3 of Ref. [21]), and the theoretical results are lower than the E706 data at $\sqrt{s}=30.6$ GeV by about a factor of 1.7 (see Fig. 4 of Ref. [21]). As mentioned above, Owens [22] has earlier explained similar discrepancies in the photon production data of $pp$, $\pi^+ p$, and $\pi^- p$ reactions at 19.4 GeV$<\sqrt{s}<63$ GeV as arising from the parton intrinsic momentum [22]. We shall provide further support of Owens' observations by analytical and numerical studies.

In this manuscript, we first examine photon production in nucleon-nucleon collisions and extend our considerations to nucleus-nucleus collisions. In nucleon-nucleus and nucleus-nucleus collisions, there are shadowing effects for photon production in nuclei. Previous experimental investigations of photon production using $\pi^-$ beams on nuclei suggest that the effective shadowing in the production of photons can be represented by a target mass dependence of the form $A^\alpha$ with $\alpha\sim 1.0$ [24], which can be explained theoretically [25]. Because $\alpha$ is close to unity, the effective shadowing for photon production in nuclei is quite weak. We shall not include the shadowing effect on photon production in nucleus-nucleus collisions.

## II. PHOTON PRODUCTION IN THE HARD-SCATTERING MODEL

In the relativistic hard-scattering process, the production of a photon in a hadron-hadron reaction ($h_a+h_b\rightarrow\gamma+X$) arises from the direct interaction of a parton of the hadron $h_a$ with a parton of the other hadron $h_b$. The basic processes are the Compton process $g+q$ (or $\overline{q}$)$\rightarrow\gamma+q$ (or $\overline{q}$), and the annihilation processes $q\overline{q}\rightarrow\gamma g$ [6–8,2].

One represents the probability for finding a parton $a$ with momentum $a=(x_a,\mathbf{a}_T)$ in the hadron $h_a$ by the parton distribution function $G_{a/h_a}(x_a,\mathbf{a}_T)$, which depends also on the momentum transfer $Q^2$. The $x_a$ and $Q^2$ dependences of the parton distribution function $G_{a/h_a}$ for various partons have been obtained by fitting large sets of experimental data in different hard-scattering processes [26–29].

In leading-order perturbative QCD, the cross section for $h_a+h_b\rightarrow\gamma+X$ is a convolution of the parton momentum distributions and their elementary collision cross sections $E_\gamma d^3\sigma(ab\rightarrow\gamma X')/dp_\gamma^3$,

$$E_\gamma\frac{d^3\sigma(h_a h_b\rightarrow\gamma X)}{dp_\gamma^3}=\sum_{ab}\int dx_a d\mathbf{a}_T dx_b d\mathbf{b}_T \times G_{a/h_a}(x_a,\mathbf{a}_T)G_{b/h_b}(x_b,\mathbf{b}_T) \times E_\gamma\frac{d^3\sigma(ab\rightarrow\gamma X')}{dp_\gamma^3}. \tag{1}$$

The parton invariant cross section is related to $d\sigma/dt$ by

$$E_\gamma\frac{d^3\sigma(ab\rightarrow\gamma X')}{dp_\gamma^3}=\frac{d\sigma(ab\rightarrow\gamma X')}{\pi dt}\delta\left(\hat{s}+\hat{t}+\hat{u}-\sum_{i=1}^{4}m_i^2\right) \times\frac{\hat{s}\sqrt{\{\hat{s}-(m_1+m_2)^2\}\{\hat{s}-(m_1-m_2)^2\}}}{(\hat{s}+m_4^2-m_3^2)}, \tag{2}$$

where $m_1$, $m_2$ are the masses of the incident partons, and $m_3$ $(=m_\gamma)$ and $m_4$ are the masses of the outgoing particles. In the above equation, we have used the Mandelstam variables

$$\hat{s}=(a+b)^2,$$
$$\hat{t}=(a-p_\gamma)^2, \tag{3}$$
$$\hat{u}=(b-p_\gamma)^2.$$

For definiteness, we shall use the nucleon-nucleon center-of-mass system to refer to the momenta of the photon and the partons. After averaging the flavors, the colors, and the isospins of the initial states of $q$, $\overline{q}$, and $g$, and summing over final states, the differential cross section $d\sigma(a+b\rightarrow\gamma+X')/dt$ are

$$\frac{d\sigma(gq\to\gamma q)}{d\hat{t}}=\frac{1}{6}\left(\frac{e_q}{e}\right)^2\frac{8\pi\alpha_s\alpha_e}{(\hat{s}-m^2)^2}\times\left\{\left(\frac{m^2}{\hat{s}-m^2}+\frac{m^2}{\hat{u}-m^2}\right)^2+\left(\frac{m^2}{\hat{s}-m^2}+\frac{m^2}{\hat{u}-m^2}\right)-\frac{1}{4}\left(\frac{\hat{s}-m^2}{\hat{u}-m^2}+\frac{\hat{u}-m^2}{\hat{s}-m^2}\right)\right\},\tag{4}$$

and

$$\frac{d\sigma(q\bar{q}\to\gamma g)}{d\hat{t}}=-\frac{4}{9}\left(\frac{e_q}{e}\right)^2\frac{8\pi\alpha_s\alpha_e}{\hat{s}(\hat{s}-4m^2)}\left\{\left(\frac{m^2}{\hat{t}-m^2}+\frac{m^2}{\hat{u}-m^2}\right)^2+\left(\frac{m^2}{\hat{t}-m^2}+\frac{m^2}{\hat{u}-m^2}\right)-\frac{1}{4}\left(\frac{\hat{t}-m^2}{\hat{u}-m^2}+\frac{\hat{u}-m^2}{\hat{t}-m^2}\right)\right\},\tag{5}$$

where $m$ is the quark mass, $e_q$ and $e$ are the quark charge and the proton charge respectively, and $\alpha_e$ and $\alpha_s$ are the electromagnetic fine-structure constant and the strong interaction coupling constant, respectively. The strong coupling constant $\alpha_s$ is related to the momentum transfer $Q^2$ by

$$\alpha_s(Q^2)=\frac{12\pi}{(33-2N_f)\ln(Q^2/\Lambda^2)},\tag{6}$$

where $N_f$ is the number of flavors, and $\Lambda$ is the QCD scale parameter.

We shall assume a factorizable parton distribution function where the intrinsic transverse momentum distribution can be factored out in the form

$$G_{a/h_a}(x_a,\mathbf{a}_T)=F_{a/h_a}(x_a,Q^2)D_a(\mathbf{a}_T).\tag{7}$$

For convenience, we normalize the transverse momentum distribution $D_a(\mathbf{a}_T)$ such that

$$\int d\mathbf{a}_T D_a(\mathbf{a}_T)=1.\tag{8}$$

Then, the function $F_{a/h_a}(x_a,Q^2)$ is the usual parton distribution function without assuming a parton intrinsic transverse momentum distribution, as given by [26–29].

## III. EFFECT OF PARTON INTRINSIC TRANSVERSE MOMENTUM

Quarks, antiquarks, and gluons are asymptotically free at high momenta, but their properties at low momenta are governed by the confinement of these particles inside a hadron. As a consequence, the transverse momentum distribution of these particles is given by their momentum wave functions. The width of the momentum distribution is related to the inverse of the size of the radius of confinement. Thus, if one takes a confinement radius of 0.5 fm, the standard deviation $\sigma$ of the parton intrinsic momentum should be of the order of $\hbar/(0.5\text{ fm})=0.4$ GeV/$c$, and the width of the intrinsic transverse momentum about $\sqrt{2}\times 0.4$ GeV/$c=0.65$ GeV/$c$. Soft gluon radiation of the partons also makes an additional contribution to the width of the intrinsic transverse momentum.

In the usual PQCD calculations, one neglects the parton intrinsic transverse momentum by approximating the parton transverse momentum distribution $D(\mathbf{a}_T)$ with a delta function $D(\mathbf{a}_T)=\delta(\mathbf{a}_T)$. Then, the integration over $\mathbf{a}_T$ and $\mathbf{b}_T$ in Eq. (1) can be trivially carried out. In such an approximate description, the colliding partons have zero transverse momentum. The produced photon acquires a transverse momentum through the basic collision processes of $gq(\text{or}\,\bar{q})\to\gamma q(\text{or}\,\bar{q})$ and $q\bar{q}\to\gamma g$, with differential distributions as given by Eqs. (4) and (5).

The transverse momentum of the photons produced from the collisions of the constituents of the quark-gluon plasma expected in high-energy heavy-ion collisions lies predominantly in the low $p_{\gamma T}$ region, extending to the region of intermediate $p_{\gamma T}$ of a few GeV/$c$. Hard-scattering processes in nucleon-nucleon collisions also produce photons in this intermediate transverse momentum region. It is necessary to determine the hard-scattering contributions to the photon production in order to extract information on the quark-gluon plasma photons. The determination of the hard-scattering photons will require the inclusion of the effects of the intrinsic parton transverse momentum.

Previously, the effect of parton intrinsic transverse momentum has been investigated by Owens [22] in hadron-nucleon collisions at different energies. In the range of 3 GeV/$c<p_{\gamma T}<8$ GeV/$c$, Owens found by numerical calculations that the parton intrinsic $p_T$ leads to an enhancement of the photon production cross section and the enhancement increases as the incident hadron energy decreases [22]. The enhancement of photon production cross section due to the parton intrinsic transverse momentum has also been reported in recent numerical calculations and experimental studies for hadron-proton collisions at $\sqrt{s}=31.7$ and 38.8 GeV [23]. It is instructive to show analytically in this section how the intrinsic transverse momentum enhances the photon production cross section. We shall make simplifying assumptions in this section in order to carry out the six-dimensional integration in Eq. (1) analytically.

We consider the production of a photon with $y_\gamma=0$ and transverse momentum $p_{\gamma T}$. We introduce the photon light-cone variable, $x_\gamma=(E_\gamma+p_{\gamma z})/\sqrt{s}$. At $y_\gamma=0$, we have $p_{\gamma z}=0$ and $x_\gamma=p_{\gamma T}/\sqrt{s}$. The photon momentum can be represented by

$$\gamma=(E_\gamma,\mathbf{p}_{\gamma T},p_{\gamma z})=(x_\gamma\sqrt{s},\mathbf{p}_{\gamma T},0).\tag{9}$$

We take the partons to be massless. The momenta of the target parton $a$ and projectile parton $b$ can be written as [see Eqs. (4.10) and (4.11) of Ref. [2]]

$$a=\left(x_a\frac{\sqrt{s}}{2}+\frac{a_T^2}{2x_a\sqrt{s}},\ \mathbf{a}_T,-x_a\frac{\sqrt{s}}{2}+\frac{a_T^2}{2x_a\sqrt{s}}\right),\tag{10}$$

$$b=\left(x_b\frac{\sqrt{s}}{2}+\frac{b_T^2}{2x_b\sqrt{s}},\ \mathbf{b}_T,x_b\frac{\sqrt{s}}{2}-\frac{b_T^2}{2x_b\sqrt{s}}\right).\tag{11}$$

The Mandelstam variables $\hat{s}$, $\hat{t}$, and $\hat{u}$ are then

$$\hat{s}=x_a x_b s+\frac{a_T^2 b_T^2}{x_a x_b s}-2\mathbf{a}_T\cdot\mathbf{b}_T, \tag{12}$$

$$\hat{u}=-\left(x_b+\frac{b_T^2}{x_b s}\right)x_\gamma s+2\mathbf{b}_T\cdot\mathbf{p}_{\gamma T}, \tag{13}$$

$$\hat{t}=-\left(x_a+\frac{a_T^2}{x_a s}\right)x_\gamma s+2\mathbf{a}_T\cdot\mathbf{p}_{\gamma T}. \tag{14}$$

The momentum conservation condition, $\hat{s}+\hat{t}+\hat{u}=0$, leads to a relation of $x_a$ in terms of $x_b$ given by

$$x_a+\frac{a_T^2}{x_a s}=x_\gamma+\frac{1}{x_b+(b_T^2/x_b s)-x_\gamma}\times\left[x_\gamma^2-\frac{2(\mathbf{a}_T+\mathbf{b}_T)\cdot\mathbf{p}_{\gamma T}-2\mathbf{a}_T\cdot\mathbf{b}_T}{s}+\frac{x_a b_T^2}{x_b s}+\frac{x_b a_T^2}{x_a s}\right].$$

To simplify the last two terms in the square bracket, we note that $x_a\sim x_b$ [see Eq. (28) below]. The above equation becomes

$$x_a+\frac{a_T^2}{x_a s}=x_\gamma+\frac{|\mathbf{p}_{\gamma T}-\mathbf{a}_T-\mathbf{b}_T|^2}{\{x_b+(b_T^2/x_b s)-x_\gamma\}s}, \tag{15}$$

which can be solved for $x_a$ to obtain $x_a=x_a(x_b)$. We assume a parton distribution function of the form $F(x)=A(1-x)^n$. The integration over the light-cone variables $x_a$ and $x_b$ in Eq. (1) becomes

$$\int dx_a dx_b A_a A_b (1-x_a)^{n_a}(1-x_b)^{n_b}\frac{\hat{s}}{\pi}\frac{d\sigma}{dt}\frac{\delta(x_a-x_a(x_b))}{s(x_b-x_\gamma)} =A_a A_b\int dx_b e^{f(x_b)}\frac{\hat{s}}{\pi s(x_b-x_\gamma)}\frac{d\sigma}{dt}, \tag{16}$$

where

$$f(x_b)=n_a\ln\{1-x_a(x_b)\}+n_b\ln(1-x_b). \tag{17}$$

The function $f(x_b)$ is an extremum of $x_b$ at

$$x_b+\frac{b_T^2}{x_b s}=x_\gamma+\sqrt{\frac{n_a(1-x_b)}{n_b(1-x_a)}}\frac{|\mathbf{p}_{\gamma T}-\mathbf{a}_T-\mathbf{b}_T|}{\sqrt{s}}. \tag{18}$$

The corresponding $x_a$ is given from Eq. (15) by

$$x_a+\frac{a_T^2}{x_a s}=x_\gamma+\sqrt{\frac{n_b(1-x_a)}{n_a(1-x_b)}}\frac{|\mathbf{p}_{\gamma T}-\mathbf{a}_T-\mathbf{b}_T|}{\sqrt{s}}. \tag{19}$$

The integration over $x_a$ and $x_b$ in Eq. (16) becomes

$$\int dx_a dx_b A_a A_b (1-x_a)^{n_a}(1-x_b)^{n_b}\frac{\hat{s}}{\pi}\frac{d\sigma}{dt}\delta(\hat{s}+\hat{t}+\hat{u}) =\sqrt{\frac{2\pi}{B}}\frac{A_a A_b\hat{s}}{\pi s(x_{bT}-x_\gamma)}(1-x_{aT})^{n_a}(1-x_{bT})^{n_b}\frac{d\sigma}{dt}, \tag{20}$$

where $x_{bT}$ and $x_{aT}$ are the solution of $x_b$ and $x_a$ from solving Eqs. (18) and (19), respectively, and $B$ is

$$B=-\left.\frac{\partial^2 f}{\partial x_b^2}\right|_{x_b=x_{bT}} =\frac{n_b}{n_a}\frac{2\sqrt{n_a n_b}(1-2x_\gamma)+x_\gamma(n_a+n_b)}{x_\gamma(1-2x_\gamma)^2}. \tag{21}$$

Consider the case with $p_{\gamma T}\gg\sigma$, where $\sigma$ is the standard deviation of the parton $p_T$ distribution. We can expand in powers of the intrinsic transverse momenta to get

$$|\mathbf{p}_{\gamma T}-\mathbf{a}_T-\mathbf{b}_T|\sim p_{\gamma T}\left(1-\frac{\mathbf{p}_{\gamma T}\cdot(\mathbf{a}_T+\mathbf{b}_T)}{p_{\gamma T}^2}\right)+\cdots. \tag{22}$$

Neglecting terms of second power in $\mathbf{a}_T$ and $\mathbf{b}_T$ and using Eqs. (18), (19), and (22), we can separate out $x_{aT}$ and $x_{bT}$ into

$$x_{iT}=x_{i0}+\Delta_i\quad(i=a,b), \tag{23}$$

where

$$x_{a0}=\left(1+\sqrt{\frac{n_b(1-x_{a0})}{n_a(1-x_{b0})}}\right)x_\gamma, \tag{24}$$

$$\Delta_a=-\sqrt{\frac{n_b(1-x_{a0})}{n_a(1-x_{b0})}}\frac{\mathbf{p}_{\gamma T}\cdot(\mathbf{a}_T+\mathbf{b}_T)}{p_{\gamma T}\sqrt{s}}, \tag{25}$$

$$x_{b0}=\left(1+\sqrt{\frac{n_a(1-x_{b0})}{n_b(1-x_{a0})}}\right)x_\gamma, \tag{26}$$

and

$$\Delta_b=-\sqrt{\frac{n_a(1-x_{b0})}{n_b(1-x_{a0})}}\frac{\mathbf{p}_{\gamma T}\cdot(\mathbf{a}_T+\mathbf{b}_T)}{p_{\gamma T}\sqrt{s}}. \tag{27}$$

For the Compton process ($gq\rightarrow\gamma q$), $n_a\sim 6$ and $n_b\sim 4$ [26], and for the annihilation process ($q\bar{q}\rightarrow\gamma g$), $n_a=n_b\sim 4$. Therefore we have approximately

$$x_{a0}\sim x_{b0}\sim 2x_\gamma. \tag{28}$$

We are now ready to carry out the integration over the intrinsic transverse momenta $\mathbf{a}_T$ and $\mathbf{b}_T$ in Eq. (1). The dependence of $(1-x_{aT})^{n_a}$ on the intrinsic momentum $\mathbf{a}_T$ can be separated out to be

$$(1-x_{aT})^{n_a}\sim(1-x_{a0})^{n_a}\exp\left\{-\frac{n_a\Delta_a}{1-x_{a0}}\right\}$$
$$\sim(1-x_{a0})^{n_a}\exp\left\{\sqrt{n_an_b}\frac{\mathbf{p}_{\gamma T}\cdot(\mathbf{a}_T+\mathbf{b}_T)}{(1-x_{a0})p_{\gamma T}\sqrt{s}}\right\}. \quad (29)$$

The factor $(1-x_{bT})^{n_b}$ can be similarly separated. The integral over the transverse momentum in Eq. (1) becomes

$$\int d\mathbf{a}_T d\mathbf{b}_T D_a(\mathbf{a}_T)D_b(\mathbf{b}_T)(1-x_{aT})^{n_a}(1-x_{bT})^{n_b}\frac{d\sigma}{dt}$$
$$=(1-2x_\gamma)^{n_a+n_b}\int d\mathbf{a}_T d\mathbf{b}_T D_a(\mathbf{a}_T)D_b(\mathbf{b}_T)$$
$$\times\exp\left\{2\sqrt{n_an_b}\frac{\mathbf{p}_{\gamma T}\cdot(\mathbf{a}_T+\mathbf{b}_T)}{(1-2x_\gamma)p_{\gamma T}\sqrt{s}}\right\}\frac{d\sigma}{dt}, \quad (30)$$

where we have used Eq. (28). We assume a Gaussian parton transverse momentum distribution, $D(\mathbf{p}_T)=\exp\{-p_T^2/2\sigma^2\}/2\pi\sigma^2$ with $\langle p_T^2\rangle=2\sigma^2$, and we obtain

$$\int d\mathbf{a}_T d\mathbf{b}_T D_a(\mathbf{a}_T)D_b(\mathbf{b}_T)$$
$$\times\exp\left\{2\sqrt{n_an_b}\frac{\mathbf{p}_{\gamma T}\cdot(\mathbf{a}_T+\mathbf{b}_T)}{(\sqrt{s}-2p_{\gamma T})p_{\gamma T}}\right\}\frac{d\sigma}{dt}$$
$$=\exp\left\{\frac{4\sigma^2n_an_b}{(\sqrt{s}-2p_{\gamma T})^2}\right\}$$
$$\times\int d\mathbf{a}_T d\mathbf{b}_T D_a(\mathbf{a}_T-\boldsymbol{\lambda})D_b(\mathbf{b}_T-\boldsymbol{\lambda})\frac{d\sigma}{dt}, \quad (31)$$

where

$$\boldsymbol{\lambda}=\frac{2\sigma^2\sqrt{n_an_b}\mathbf{p}_{\gamma T}}{(\sqrt{s}-2p_{\gamma T})p_{\gamma T}}. \quad (32)$$

The first factor on the right-hand side of Eq. (31),

$$\kappa_1=\exp\left\{\frac{4\sigma^2n_an_b}{(\sqrt{s}-2p_{\gamma T})^2}\right\}, \quad (33)$$

is the enhancement factor due to the parton intrinsic transverse momentum and the variation of the parton distribution function. We can understand the origin of this enhancement in the following way. The integration over $x_a$ and $x_b$ leads to a cross section proportional to $(1-x_{aT})^{n_a}(1-x_{bT})^{n_b}$ [Eq. (20)]. If there were no parton intrinsic transverse momentum, $x_{aT}$ would be given by $x_{a0}$. The presence of the intrinsic transverse momentum leads to $x_{aT}$ varying about $x_{a0}$ with the variation $\Delta_a$ depending on the intrinsic transverse momentum [Eq. (23)]. Because of the steep decrease of $(1-x_a)^{n_a}(1-x_b)^{n_b}$ as a function of $x_a$ and $x_b$, the averaging over the transverse momenta leads to the enhancement factor $\kappa_1$.

The enhancement factor $\kappa_1$ arising from the parton distribution function allows us to determine the scale of $p_{\gamma T}$ at which the effect of the parton intrinsic $p_T$ will be important. The enhancement factor $\kappa_1$ is close to unity if $4\sigma^2n_an_b \ll(\sqrt{s}-2p_{\gamma T})^2$ and is much greater than unity if $4\sigma^2n_an_b$ is large or comparable to $(\sqrt{s}-2p_{\gamma T})^2$. As $n_an_b\sim24$ for the Compton process, the importance of the intrinsic $p_T$ depends on whether $7\sqrt{2}\sigma$ is small compared to $\sqrt{s}-2p_{\gamma T}$. When $7\sqrt{2}\sigma$ is large or comparable to $(\sqrt{s}-2p_{\gamma T})$, the enhancement factor $\kappa_1$ becomes quite large. This is the main origin for the large enhancement factor for $p_{\gamma T}<6$ GeV/$c$ in hadron-proton collisions at $\sqrt{s}\sim20$ GeV.

For the cross section $d\sigma/dt$, the dominant contributions come from terms proportional to $1/\hat{t}$ and $1/\hat{u}$. It can be approximated by

$$\frac{d\sigma}{dt}\sim C\left(\frac{1}{\hat{t}}+\frac{1}{\hat{u}}\right). \quad (34)$$

From Eqs. (13), (14), and (28), we have

$$\hat{t}\sim|\mathbf{p}_{\gamma t}-\mathbf{b}_T|^2, \quad (35)$$

and

$$\hat{u}\sim|\mathbf{p}_{\gamma t}-\mathbf{a}_T|^2. \quad (36)$$

The integration over the intrinsic transverse momentum distributions can be carried out to yield

$$\int d\mathbf{a}_T d\mathbf{b}_T D_a(\mathbf{a}_T-\boldsymbol{\lambda})D_b(\mathbf{b}_T-\boldsymbol{\lambda})C$$
$$\times\left(\frac{1}{(\mathbf{p}_{\gamma_T}-\mathbf{a}_T)^2}+\frac{1}{(\mathbf{p}_{\gamma_T}-\mathbf{b}_T)^2}\right)$$
$$\sim\left\{\frac{p_{\gamma_T}^2}{(\mathbf{p}_{\gamma_T}-\boldsymbol{\lambda})^2-2\sigma^2}\right\}\frac{2C}{p_{\gamma T}^2}, \quad \text{for } p_{\gamma T}\gg\sigma \quad (37)$$

where first factor on the right-hand side

$$\kappa_2=\frac{p_{\gamma T}^2}{(\mathbf{p}_{\gamma T}-\boldsymbol{\lambda})^2-2\sigma^2}, \quad (38)$$

is the enhancement factor due to the parton intrinsic transverse momentum and the variation of $d\sigma/dt$. This enhancement factor $\kappa_2$ arising from $d\sigma/dt$ is close to unity if $p_{\gamma T}\gg\sigma$. From Eqs. (34), (35), and (36), the enhancement factor due to $d\sigma/dt$ becomes much greater than unity when $p_{\gamma T}$ is of the order $\sigma$.

Putting all the results together, we have

$$E_\gamma\frac{d^3\sigma(h_ah_b\to\gamma X)}{dp_\gamma^3}\sim\kappa\sqrt{\frac{2\pi}{B}}\frac{4A_aA_bp_{\gamma T}}{\pi\sqrt{s}}$$
$$\times\left(1-\frac{2p_{\gamma T}}{\sqrt{s}}\right)^{n_a+n_b}\frac{2C}{p_{\gamma T}^2}, \quad (39)$$

where $\kappa$ is given by

$$\kappa=\kappa_1\kappa_2=\exp\left\{\frac{4\sigma^2 n_a n_b}{(\sqrt{s}-2p_{\gamma T})^2}\right\}\frac{p_{\gamma T}^2}{p_{\gamma T}^2(1-\lambda)^2-2\sigma^2}. \tag{40}$$

The quantity $\kappa$ in Eqs. (39) and (40) is the ratio of the photon production cross section with the parton intrinsic transverse momentum to the cross section without the parton intrinsic transverse momentum. From Eq. (40) we infer that for $p_{\gamma T}\gg\sqrt{\langle p_T^2\rangle}$, which allows the expansion in Eq. (22), $\kappa$ is greater than unity and represents an enhancement due to the parton intrinsic transverse momentum. It is a function of both $\sqrt{s}$ and $p_{\gamma T}$. It decreases as $\sqrt{s}$ increases. For the same $\sqrt{s}$, the first factor increases with increasing $p_{\gamma T}$ while the second factor increases with decreasing $p_{\gamma T}$.

If one uses $2\sigma^2=0.9$ (GeV/$c$)$^2$ as given by Owens [22], then for $p_{\gamma T}=6$ GeV/$c$ at $\sqrt{s}=20$ GeV, Eqs. (33) and (38) give $\kappa_1=2.2$ and $\kappa_2=1.27$, and a combined enhancement factor $\kappa=2.8$, in rough agreement with the enhancement factor of about 3.8 obtained from numerical calculations in Fig. 3. There is a substantial enhancement of the photon production cross section at $\sqrt{s}\sim 20$ GeV due to the parton intrinsic transverse momentum. For $p_{\gamma T}=6$ GeV/$c$ at $\sqrt{s}=63$ GeV, $\kappa$ decreases to 1.07, in agreement with the numerical results in Fig. 4. This value of $\kappa$ is only slightly greater than unity, indicating that the parton intrinsic $p_T$ has only small influence for $p_{\gamma T}\sim 6$ GeV/$c$ at $\sqrt{s}>63$ GeV.

The enhancement factor $\kappa$ in Eq. (40) shows that one should expect a large enhancement due to the intrinsic transverse momentum for the production of photons with transverse momentum $p_{\gamma T}$ close to $\sqrt{s}/2$ such that $\sqrt{s}-2p_{\gamma T}$ is not much greater than $\sqrt{\langle p_T^2\rangle}$. In this case, $x_{a0}\sim 2p_{\gamma T}/\sqrt{s}$ is close to unity and the magnitude of the cross section is however quite small.

The above analytical integration of the six-dimensional integral of Eq. (1) serves the purpose of illustrating the important features of the enhancement due to the parton intrinsic transverse momentum. In order to compare with experimental data quantitatively, we need to carry out numerical integrations of Eq. (1) in their full complexities without simplifying assumptions in the following sections.

## IV. TRANSVERSE MOMENTUM DISTRIBUTION OF PARTONS

The momentum distribution of partons for small $p_T$ depends on confinement, while the momentum distribution at high $p_T$ depends on the constituent counting rule which is a power law in nature [30,31,2]. They have different functional forms. To carry out our investigation of the parton intrinsic momentum in numerical calculations, we join the two different functional forms at $p_{TM}$ and assume the parton $p_T$ distribution function of the form

$$D(\mathbf{p}_T)=C\left[\frac{1}{1+e^{(p_T-p_{TM})/\Delta}}D_1(p_T)+\frac{1}{1+e^{(p_{TM}-p_T)/\Delta}}D_2(p_T)\right], \tag{41}$$

where $C\sim 1$ will be determined by the normalization condition Eq. (8).

Following Owens [22], we use the Gaussian distribution $D_1(\mathbf{p}_T)$ for the distribution at low $p_T$ as given by

$$D_1(p_T)=\frac{1}{2\pi\sigma^2}e^{-p_T^2/2\sigma^2}. \tag{42}$$

For large $p_T$, we take the transverse momentum distribution $D_2(p_T)$ to be given by a power-law distribution as in the spectator counting rule of Blankenbecler and Brodsky [30]

$$D_2(p_T)=\frac{a}{(p_T^2+M^2)^n}, \tag{43}$$

where $a=D_1(p_{TM})(p_{TM}^2+M^2)^n$. The results of our calculation for photon production are rather insensitive to this transverse distribution $D_2$. Using information from the work of Sivers, Blankenbecler, and Brodsky [31], we choose $n=4$ and $M=1$ GeV to describe the transverse momentum distribution $D_2$. For numerical purposes, we set the matching transverse momentum to be $p_{TM}=2\sqrt{2}\sigma$, and the matching width $\Delta=0.25$ GeV/$c$.

## V. NEXT-TO-LEADING-ORDER PERTURBATIVE QCD

It is well known that higher-order perturbative QCD corrections are important in the evaluation of the cross sections for many hard-scattering processes (see for example, Refs. [32] and [27]). For photon production, contributions up to the second order in $\alpha_s$ have been considered by Aurenche, Baier, Douiri, Fontannaz, and Schiff, and by Baer, Ohnemus, and Owens [18–20]. These calculations involve the evaluation of contributions from all next-to-leading-order Feynman diagrams. In these calculations [18–20], the intrinsic transverse momentum of the partons has been neglected by using a delta function distribution $\delta(\mathbf{p}_T)$ so that integrations over the transverse momentum of the partons can be trivially carried out. From these leading-order plus next-to-leading-order (LO+NLO) calculations, the effects of the higher-order terms can be represented by the $K$-factor defined by

$$K(p_\gamma)=\left\{E_\gamma\frac{d^3\sigma}{dp_\gamma^3}(\mathrm{LO+NLO})\Big/E_\gamma\frac{d^3\sigma}{dp_\gamma^3}(\mathrm{LO})\right\}, \tag{44}$$

where $E_\gamma(d^3\sigma/dp_\gamma^3)(\mathrm{LO+NLO})$ is the photon obtained with the inclusion of both the lowest-order and the next-to-leading-order terms, and $E_\gamma(d^3\sigma/dp_\gamma^3)(\mathrm{LO})$ is the photon cross section obtained in the lowest-order calculation.

Numerically, the $K$-factor is about 2 to 3.5 and is a slowly varying function of the photon transverse momentum (see Figs. 1 and 2). It represents an effective modification of the strength of the coupling constant at the vertex, as in a vertex

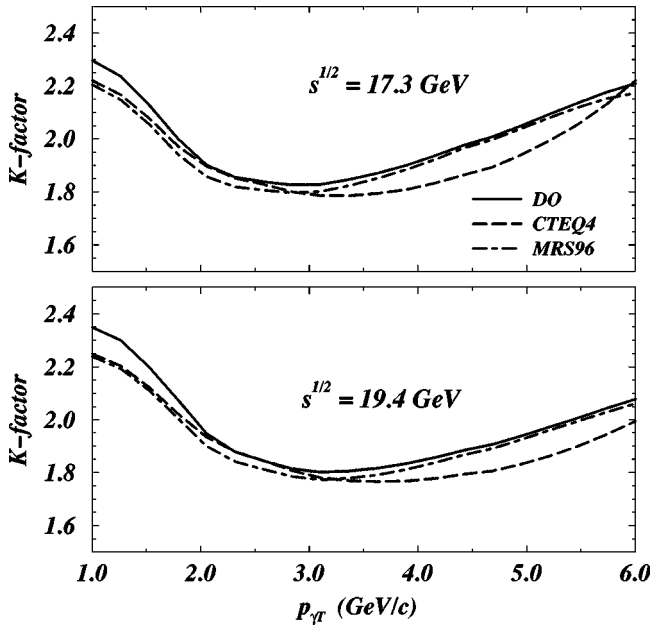


FIG. 1. The $K$-factor as a function of the photon transverse momentum $p_{\gamma T}$ at $y_\gamma=0$. (a) for $pp$ collisions at $\sqrt{s}=17.3$ GeV and (b) for $\sqrt{s}=19.4$ GeV.

correction, due to the initial-state interaction between partons [32–35]. On the other hand, the vertex correction depends on the relative momentum between the colliding partons [33–35], which in turn depends mainly on the longitudinal momenta; the vertex correction is insensitive to the parton transverse momenta. Because of this property, it is reasonable to consider the $K$-factor to be approximately independent of the parton transverse momentum; that is

$$\left\{ E_\gamma \frac{d^3\sigma}{dp_\gamma^3}(\mathrm{LO+NLO+PT}) \Big/ E_\gamma \frac{d^3\sigma}{dp_\gamma^3}(\mathrm{LO+PT}) \right\} \sim \left\{ E_\gamma \frac{d^3\sigma}{dp_\gamma^3}(\mathrm{LO+NLO}) \Big/ E_\gamma \frac{d^3\sigma}{dp_\gamma^3}(\mathrm{LO}) \right\}, \tag{45}$$

where the abbreviation ''PT'' stands for calculations where the parton transverse momentum distribution is taken into account. Upon using the above approximation to include the effects of the next-to-leading-order corrections and the parton intrinsic transverse momentum distribution, the photon production cross section is given by

$$E_\gamma \frac{d^3\sigma}{dp_\gamma^3}(\mathrm{LO+NLO+PT}) \sim K(p_\gamma) E_\gamma \frac{d^3\sigma}{dp_\gamma^3}(\mathrm{LO+PT}). \tag{46}$$

## VI. PHOTON PRODUCTION IN NUCLEON-NUCLEON COLLISIONS

From Eq. (46), we can take into account the effects of intrinsic transverse momentum and next-to-leading-order contributions by carrying out the calculation in two steps. We perform the LO+NLO calculations, without the intrinsic parton transverse momentum distribution, using the numerical code from Aurenche *et al.* [18,19]. The ratio of the LO+NLO calculation to the leading-order (LO) calculation then gives the $K$-factor as a function of the photon momentum, as defined by Eq. (44). We then carry out separately a numerical calculation of the leading order with the intrinsic transverse momentum distribution. Equation (46) is then used to give the cross section when both effects are included.

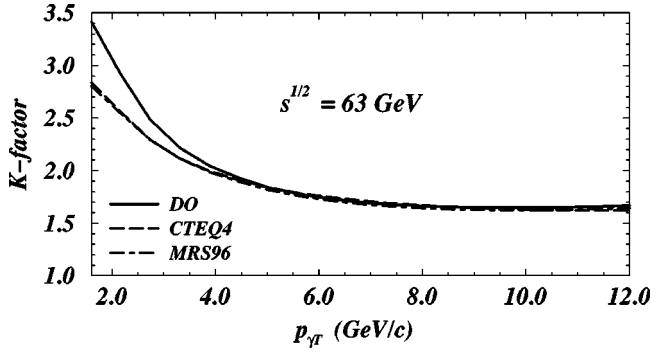


FIG. 2. The $K$-factor as a function of the photon transverse momentum $p_{\gamma T}$ at $y_\gamma=0$ for $pp$ collisions at $\sqrt{s}=63$ GeV.

The photon cross section depends on the functional dependence of $Q^2$ in terms of physical quantities such as $p_{\gamma T}$ of the photon. Owens has studied different choices of the functional form, from $Q^2=p_{\gamma T}^2$ to $Q^2=p_{\gamma T}^2/4$, and found that $Q^2=p_{\gamma T}^2/2$ gives the best description of the experimental data for production of photons with large transverse momenta [22]. We shall accordingly use this functional dependence for our investigation.

We first carry out the LO and the LO+NLO calculations using three different parton distribution functions: (1) the Duke and Owens parton distribution function (set 1) [26], (2) the CTEQ4 parton distribution function (set 3) [27,28], and (3) the MRS96 parton distribution function (set 1) [29]. The ratio of the LO+NLO result to the LO result gives the $K$-factors which are shown in Figs. 1 and 2, and the results for LO and LO+NLO cross sections are shown in Figs. 5 and 6. The $K$-factor in Figs. 1 and 2 as a function of the photon transverse momentum $p_{\gamma T}$ for $y_\gamma=0$ indicate that it has a value of approximately 2 for 1 GeV/$c<p_{\gamma T}<6$ GeV/$c$ in nucleon-nucleon collisions at $\sqrt{s}=17.3$ and 19.4 GeV. It behaves slightly differently for $\sqrt{s}=63$ GeV, where it drops from about 3 to 1.4, as $p_{\gamma T}$ decreases from 2 GeV/$c$ to 6 GeV/$c$. It becomes nearly a constant for $p_{\gamma T}>6$ GeV/$c$.

We next carry out a lowest-order calculation with the inclusion of the transverse momentum distribution of the partons. Previously, Owens noted that the transverse momentum distribution of dilepton pairs gives a direct measure of the parton intrinsic transverse momentum [22]. Data obtained by Kaplan *et al.* [36] for $pp$ collisions at $\sqrt{s}=27.4$ GeV indicate $\langle p_T^2(\mu^+\mu^-)\rangle=1.9$ (GeV/$c$)$^2$ which corresponds to a parton transverse momentum $2\sigma^2=0.95$ (GeV/$c$)$^2$ in the lowest order approximation. The value of $\sigma$ decreases if higher-order terms are included [32]. The convolution method of Ref. [32] is however a model-dependent prescription for incorporating the effects of the intrinsic transverse momentum. Nevertheless, it indicates that the amount of intrinsic transverse momentum needed to describe the data is influenced by the amount of QCD dynamics included in the analysis. The analysis of Owens using the lowest-order QCD with a constant $K$-factor indicates that $\langle p_T^2\rangle=2\sigma^2=0.9$

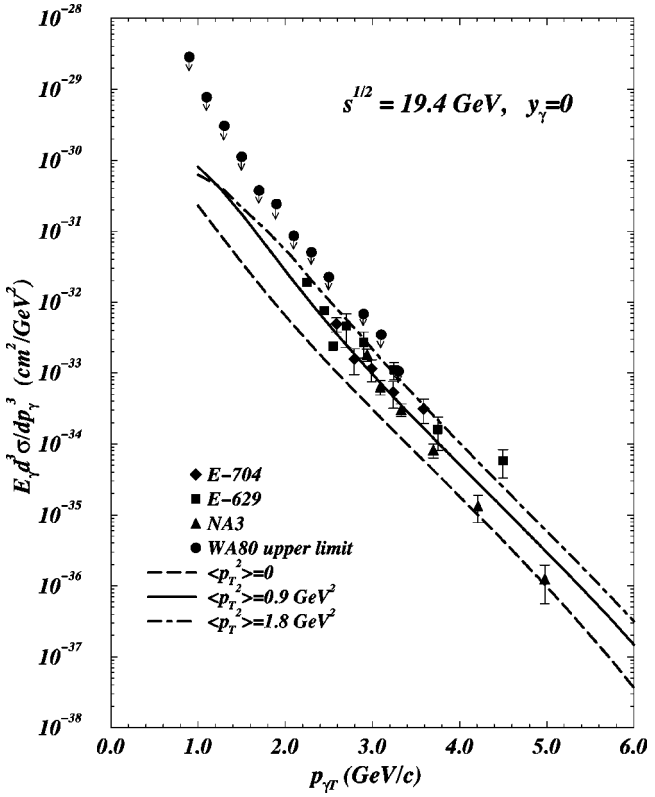


FIG. 3. The photon invariant cross section for nucleon-nucleon collisions at $\sqrt{s}=19.4$ GeV and $y_\gamma=0$ calculated with different $\langle p_T^2\rangle=2\sigma^2$ values of parton intrinsic momentum distribution and the Duke and Owens parton distribution function (set 1). The NLO corrections have been included according to Eqs. (44) and (46).

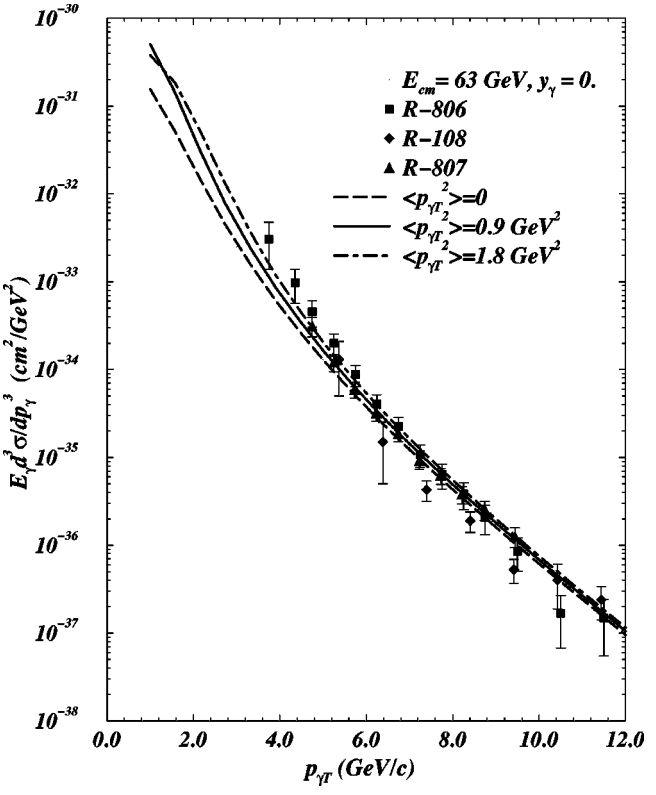


FIG. 4. The photon invariant cross section for nucleon-nucleon collisions at $\sqrt{s}=63$ GeV and $y_\gamma=0$ calculated with different $\langle p_T^2\rangle$ values of parton intrinsic momentum distribution and the Duke and Owens parton distribution function (set 1). The NLO corrections have been included.

$(\mathrm{GeV}/c)^2$ gives a good agreement with photon production data in $pp$, $\pi^+p$, and $\pi^-p$ collisions at 19.4 GeV$<\sqrt{s}<62$ GeV [22]. Recent analysis [23] suggests even a greater value of $\langle p_T^2\rangle$ of about 2 $(\mathrm{GeV}/c)^2$. More future work is needed to clarify the situation on the magnitude of the parton intrinsic transverse momentum.

To see the dependence of the photon transverse momentum distribution on the magnitude of $\langle p_T^2\rangle$ of the parton intrinsic transverse momentum, we show in Fig. 3 the results for $pp$ collisions at $\sqrt{s}=19.4$ GeV, using the Duke and Owens parton distribution function (set 1). The cross sections for $\sigma=0$ are less than those for $\langle p_T^2\rangle=2\sigma^2=0.9$ $(\mathrm{GeV}/c)^2$ by about a factor of 3 to 4, which are less than those for $\langle p_T^2\rangle=2\sigma^2=1.8$ $(\mathrm{GeV}/c)^2$ by about a factor of 2 (except at $p_{\gamma T}\simeq 1$ GeV/$c$). There is a substantial enhancement of the cross section due to the parton intrinsic transverse momenta. The value of $\langle p_T^2\rangle=2\sigma^2=0.9$ $(\mathrm{GeV}/c)^2$ provides a good description of the experimental data. The enhancement factor for $\langle p_T^2\rangle=2\sigma^2=0.9$ $(\mathrm{GeV}/c)^2$ is relatively constant for $\sqrt{s}\sim 20$ GeV.

The enhancement of the photon production cross section in the region of $p_{\gamma T}$ under consideration poses an interesting puzzle. If the running coupling constant could be taken as a fixed constant, the total cross section obtained by integrating the photon momentum should be independent of the width (or $\sigma$) of the parton intrinsic transverse momentum distribution. An enhancement of the cross sections in all regions of $p_{\gamma T}$ appears to violate this normalization of the total photon production cross section. The puzzle is resolved by noting that the cross section is not enhanced in all regions of $p_{\gamma T}$. The photon production cross section is enhanced in the region $p_{\gamma T}\gg\sigma$, and it is suppressed for $p_{\gamma T}\ll\sigma$ because partons acquire energies through their intrinsic $p_T$ and the probability for producing very low energy photons therefore decreases when partons have intrinsic $p_T$. A hint of the suppression for low $p_{\gamma T}$ can be found in Figs. 3 and 4 where for $p_{\gamma T}<1.2$ GeV/$c$ the cross section for the case $2\sigma^2=1.8$ $(\mathrm{GeV}/c)^2$ is lower than that for $2\sigma^2=0.9$ $(\mathrm{GeV}/c)^2$. While we expect a suppression for this region of small $p_{\gamma T}\ll\sigma$, it is a different matter whether perturbative QCD can remain valid for this region where the associated value of $Q^2$ becomes very small. We shall not consider this region of small $p_{\gamma T}$.

Figure 4 shows the direct photon production results for nucleon-nucleon collisions at $\sqrt{s}=63$ GeV and $y_\gamma=0$. The nucleon-nucleon collision data from R806/807 [40] and R108 (CCOR) Collaborations [41] are shown in the figure. For $p_{\gamma T}>1.2$ GeV/$c$, the cross section is enhanced as $\sigma$ increases. The magnitude of the enhancement is smaller than that for $\sqrt{s}=19.4$ GeV, indicating that the effect of intrinsic transverse momentum decreases with increasing $\sqrt{s}$. For $p_{\gamma T}<1.2$ GeV/$c$, the cross section initially increases as $\sigma$ increases but decreases as $\langle p_T^2\rangle$ increases further, indicating that the trend of enhancement is reversed for $p_{\gamma T}\ll\sigma$. The value of $2\sigma^2=0.9$ $(\mathrm{GeV}/c)^2$ provides a good description of the experimental data. We shall henceforth follow

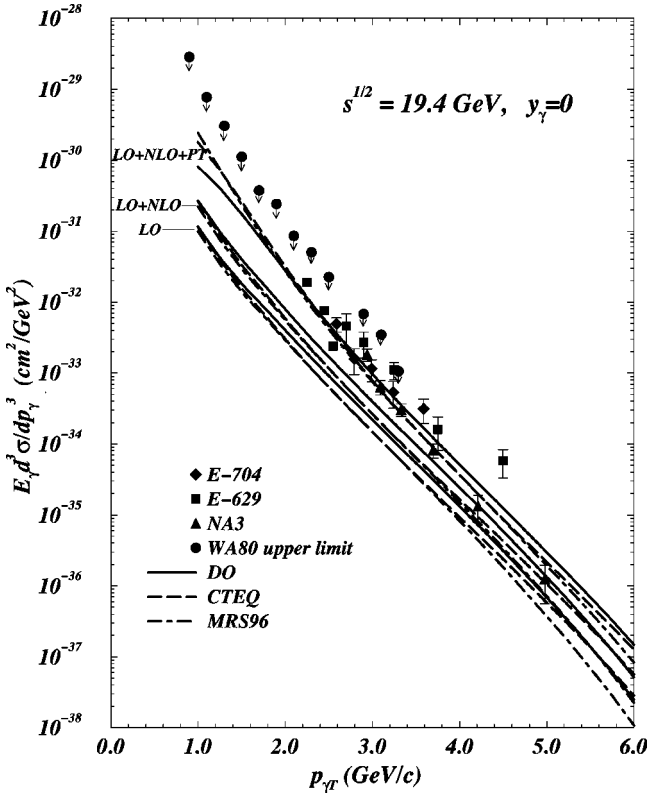


FIG. 5. The photon invariant cross section for nucleon-nucleon collisions at $\sqrt{s}=19.4$ GeV and $y_\gamma=0$.

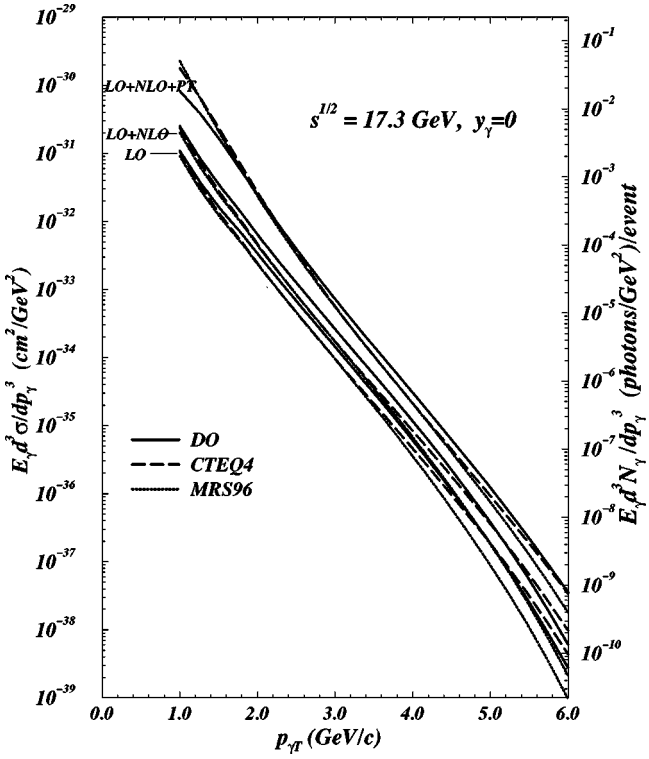


FIG. 6. The photon invariant cross section for nucleon-nucleon collisions at $\sqrt{s}=17.3$ GeV and $y_\gamma=0$. The scale on the right refers to the photon distribution per central Pb-Pb collision event in the WA98 measurement (Ref. [12]).

Owens [22] to use $2\sigma^2=0.9$ (GeV/$c$)$^2$ when we include the parton intrinsic transverse momentum distribution in our subsequent calculations.

In Fig. 5 we present results of the photon cross section for the LO calculations, the LO+NLO calculations, and the LO +NLO+PT results including further the effect of the transverse momentum distribution, for $pp$ collisions at $\sqrt{s}=19.4$ GeV and $y_\gamma=0$. The LO+NLO calculations are enhanced from the LO calculations by about a factor of 2, and the intrinsic momentum effect brings another factor of about 4 to 8, depending on the parton distribution function. The intrinsic transverse momentum of partons enhances the cross sections by a substantial factor and is very important in the region of intermediate $p_{\gamma T}$. The data for $\sqrt{s}=19.4$ GeV from E704 [37], E629 [38], and NA3 [39] are also shown in Figs. 3 and 5. (The NA3 data are taken from the reaction $p+{}^{12}C\rightarrow\gamma+X$ where we assume a nuclear dependence of $A^{1.0}$, as in Ref. [37].) The WA80 data in Figs. 3 and 5 represent the upper limits of the cross section. The experimental data in the region of $p_{\gamma T}$ from 2 to 4 GeV/$c$ can be described well when both the effects of higher-order terms and the parton intrinsic transverse momentum are taken into account. For the region $p_{\gamma T}>4$ GeV/$c$, the experimental data of NA3 and E629 are different. The data of NA3 above 4 GeV/$c$ fall within the predictions using the CTEQ4 and the MRS96 parton distribution functions. Within the considerable experimental uncertainties, the experimental data agree with the LO+NLO+PT predictions, although there are small differences in the results from different parton distribution functions.

Recent photon production experiments using high-energy heavy ions were performed for Pb-Pb collisions at 158 GeV per nucleon [12,13], which correspond to nucleon-nucleon collisions at $\sqrt{s}=17.3$ GeV. In order to facilitate the comparison with experimental data, we show the theoretical results for $pp$ collisions at $\sqrt{s}=17.3$ GeV and $y_\gamma=0$ in Fig. 6. The intrinsic transverse momentum enhances the cross sections by a factor of about 4 to 8. It is therefore an important effect which must be included in the discussion of photon cross sections in the region of $p_{\gamma T}$ between 1 and 6 GeV/$c$.

## VII. PHOTON PRODUCTION FROM THE QCD HARD-SCATTERING PROCESSES IN NUCLEUS-NUCLEUS COLLISIONS

We can determine the direct photon production cross section in high-energy nucleus-nucleus collisions arising from the hard scattering between partons. Because of the weak effective shadowing effect in photon production by parton collisions as indicated by experimental $p$A data [24], we shall neglect the shadowing effect. The photon distribution in a collision of a nucleus $A$ and a nucleus $B$ at an impact parameter **b** due to the hard scattering of partons is given by

$$E_\gamma\frac{dN_\gamma^{AB}(\mathrm{HS})}{d\mathbf{p}_\gamma}(\mathbf{b})=n_{NN}(\mathbf{b})E_\gamma\frac{dN_\gamma^{NN}(\mathrm{HS})}{d\mathbf{p}_\gamma}, \qquad (47)$$

where $n_{NN}(b)$ is the number of inelastic nucleon-nucleon collisions,

$$n_{NN}(\mathbf{b})=ABT_{AB}(\mathbf{b})\sigma_{in}^{NN}, \qquad (48)$$

and the photon distribution in an inelastic nucleon-nucleon collision is

$$E_\gamma \frac{dN_\gamma^{NN}(\mathrm{HS})}{d\mathbf{p}_\gamma} = E_\gamma \frac{d\sigma_\gamma^{NN}(\mathrm{HS})}{\sigma_{in}^{NN} d\mathbf{p}_\gamma}. \quad (49)$$

In the above equations, $\sigma_{in}^{NN}$ and $\sigma_\gamma^{NN}$ are the nucleon-nucleon total inelastic cross section and photon production cross section respectively, $T_{AB}(\mathbf{b})$ is the thickness function for the nucleus-nucleus collision [2]

$$T_{AB}(\mathbf{b}) = \int d\mathbf{b}_A d\mathbf{b}_B T_A(\mathbf{b}_A) T_B(\mathbf{b}_B) t(\mathbf{b}-\mathbf{b}_A-\mathbf{b}_B), \quad (50)$$

where $T_A(\mathbf{b})$ and $T_B(\mathbf{b})$ are respectively the thickness functions for nucleus $A$ and $B$, and the baryon-baryon thickness function $t(\mathbf{b}-\mathbf{b}_A-\mathbf{b}_B)$ can be approximated by a delta function, $t(\mathbf{b}-\mathbf{b}_A-\mathbf{b}_B)=\delta(\mathbf{b}-\mathbf{b}_A-\mathbf{b}_B)$. Note that when one combines Eqs. (47), (48), and (49), the nucleon-nucleon inelastic cross section $\sigma_{in}^{NN}$ cancels out and one obtains the result

$$E_\gamma \frac{dN_\gamma^{AB}(\mathrm{HS})}{d\mathbf{p}_\gamma}(\mathbf{b}) = ABT_{AB}(\mathbf{b}) E_\gamma \frac{d\sigma_\gamma^{NN}(\mathrm{HS})}{d\mathbf{p}_\gamma}. \quad (51)$$

Writing the result for nucleus-nucleus collisions in the form of Eq. (47) provides a more intuitive picture of the scaling of the photon multiplicity from nucleon-nucleon collisions to nucleus-nucleus collisions.

Experimentally, one measures the yield of photons per event of nucleus-nucleus collisions in coincidence with the measurement of the degree of inelasticity of the events, as characterized by the multiplicity of produced particles. Results are given in terms of the photon yield per inelastic collision event for the most-inelastic fraction $f$ of all inelastic events. The most-inelastic fraction $f$ depends on the maximum impact parameter $b_m$, and one can deduce a relation of $f$ as a function of the maximum impact parameter $b_m$ from the Glauber model by

$$f(b_m) = \frac{\int_o^{b_m} d\mathbf{b}\{1-(1-T_{AB}(\mathbf{b})\sigma_{in}^{NN})^{AB}\}}{\int_o^{\infty} d\mathbf{b}\{1-(1-T_{AB}(\mathbf{b})\sigma_{in}^{NN})^{AB}\}}. \quad (52)$$

For measurements within the most-inelastic fraction $f(b_m)$ of events, the photon distribution per inelastic event is given by taking the average of Eq. (47) over the range of impact parameters from 0 to $b_m$. We therefore have the photon distribution per inelastic event in a nucleus-nucleus collision given by

$$E_\gamma \frac{dN_\gamma^{AB}(\mathrm{HS})}{d\mathbf{p}_\gamma}(b_m) = \langle n_{NN}\rangle(b_m) E_\gamma \frac{d\sigma_\gamma^{NN}(\mathrm{HS})}{\sigma_{in}^{NN} d\mathbf{p}_\gamma}, \quad (53)$$

where the average number of nucleon-nucleon collisions per event within the range of impact parameters from 0 to $b_m$ is

$$\langle n_{NN}\rangle(b_m) = \frac{\int_0^{b_m} d\mathbf{b} ABT_{AB}(\mathbf{b})\sigma_{in}^{NN}}{\int_o^{b_m} d\mathbf{b}\{1-\left(1-T_{AB}(\mathbf{b})\sigma_{in}^{NN}\right)^{AB}\}}. \quad (54)$$

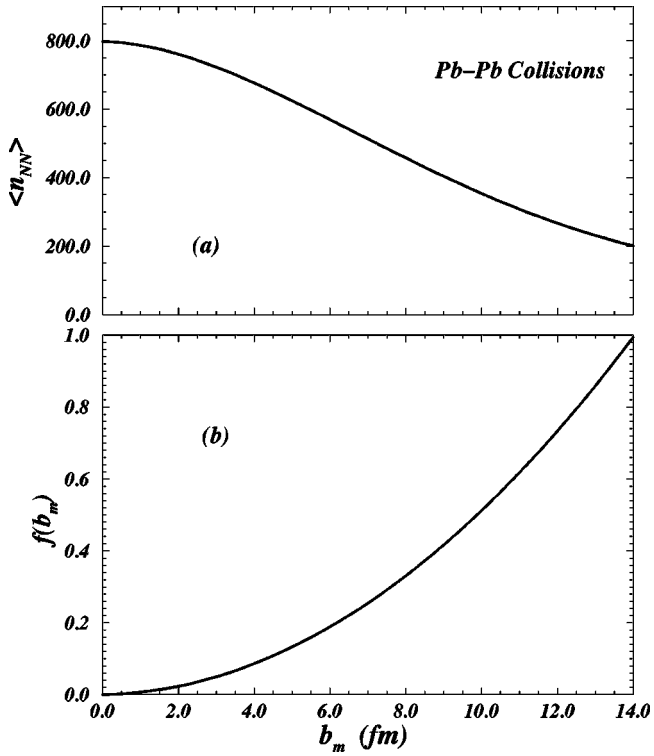


FIG. 7. (a) The number of inelastic nucleon-nucleon collisions in Pb-Pb collisions averaged over the impact parameter from 0 to $b_m$ as a function of the impact parameter $b_m$. (b) The fraction of the total inelastic cross section for collisions with an impact parameter from 0 to $b_m$.

In Fig. 7(a) we show $\langle n_{NN}\rangle(b_m)$, the number of nucleon-nucleon inelastic collisions averaged over the range $0<b<b_m$, as a function of the maximum impact parameter $b_m$ for Pb-Pb collisions, and in Fig. 7(b) the corresponding most-inelastic fraction $f(b_m)$.

The photon production data from the WA98 Collaboration were collected for the most-inelastic 10% of the total number of Pb-Pb inelastic collisions [12]. For this value of $f(b_m)=0.1$, the impact parameter $b_m$ is found from Fig. 7 to be 4.44 fm. With an inelastic nucleon-nucleon cross section of 29.4 mb [2], the average number of inelastic nucleon-nucleon collisions within this range of impact parameters from 0 to 4.44 fm is $\langle n_{NN}\rangle=654$. This is the scaling number which one must multiply to the photon yield in a nucleon-nucleon inelastic collision to give the total photon yield per central Pb-Pb collision.

Using this scaling factor, we obtain the photon distribution from hard scattering of partons per central Pb-Pb collision at a nucleon-nucleon collision energy of $\sqrt{s}=17.3$ GeV and $y_\gamma=0$. They are shown as the dashed and dashed-dot curve in Fig. 8 for the CTEQ4 parton distribution function (set 3) and the MRS96 parton distribution function (set 1). They have been calculated for the most-inelastic 10% of the inelastic Pb-Pb collisions. They should be compared with photon distributions from the quark-gluon plasma at different temperatures to be discussed in the next section and shown as the solid curves in Fig. 8.

The scaling between nucleon-nucleon collisions to nucleus-nucleus collisions can be extended for S-Au colli-

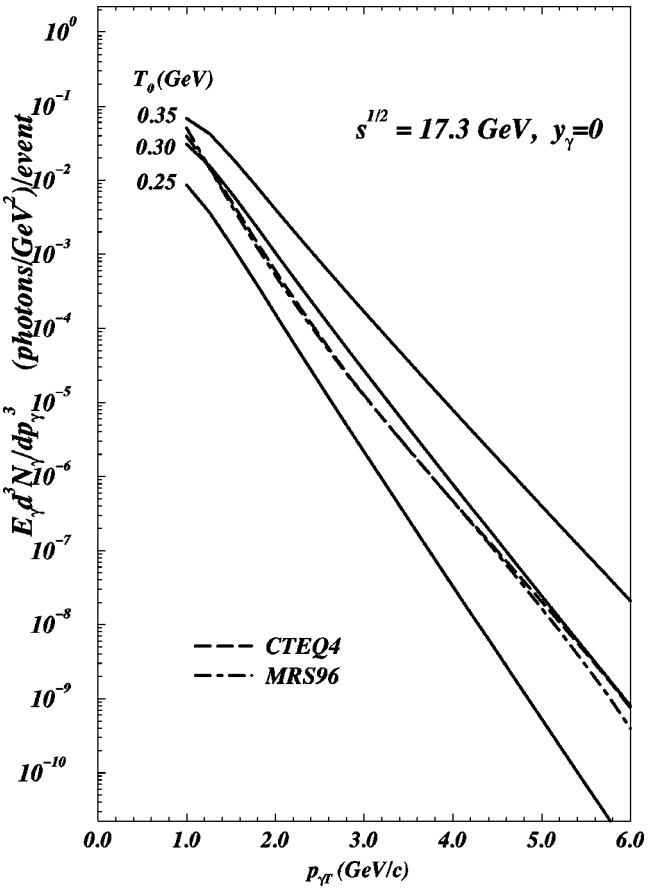


FIG. 8. The invariant photon distribution per central Pb-Pb collision event in the WA98 measurement (Ref. [12]) at $y_\gamma=0$ as a function of $p_{\gamma T}$. The dashed and dashed-dot curves are results from parton hard scattering obtained in LO+NLO+PT calculations, and the solid curves are from a quark-gluon plasma with different initial temperatures $T_0$ and a critical temperature $T_c=200$ MeV.

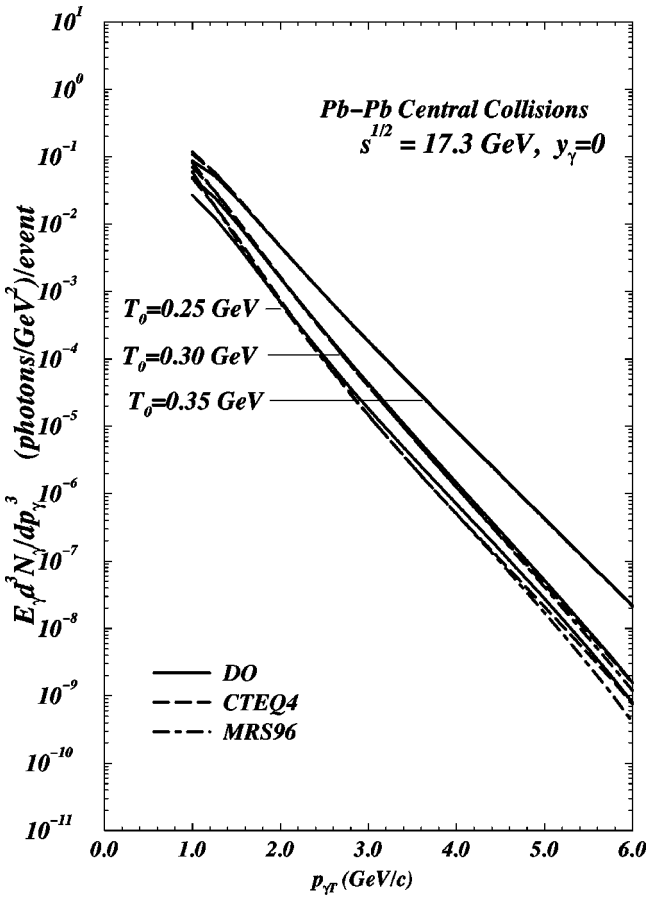


FIG. 9. The total invariant photon distribution per central Pb-Pb collision event in the WA98 measurement at $y_\gamma=0$ as a function of $p_{\gamma T}$, including the contributions from nucleon-nucleon hard scatterings and the quark-gluon plasma with an initial temperature $T_0$.

sions which were studied by the WA80 Collaboration [11]. The WA80 photon data were collected for the 7.4% of the most-inelastic events for which the maximum impact parameter $b_m$ is found to be 2.9 fm and the number of nucleon-nucleon inelastic collisions $\langle n_{NN}\rangle$ averaged over the range of impact parameters from 0 to $b_m$ is 160. This scaling number has been used to convert the WA80 upper limit $E_\gamma dN_\gamma^{SAu}/d^3p_\gamma$ data to $E_\gamma d\sigma_\gamma^{NN}/d^3p_\gamma$ data in Figs. 3 and 5.

## VIII. PHOTON PRODUCTION FROM THE QGP IN NUCLEUS-NUCLEUS COLLISIONS

In a quark-gluon plasma, the constituents of the plasma interact with each other. The interaction between the constituents leads to the production of photons via $gq$ (or $g\bar{q}$) $\rightarrow \gamma q$ (or $q\bar{q}$) and $q\bar{q}\rightarrow \gamma g$ reactions, which are the same processes as in photon production in parton collisions [6–10,14]. Upon taking the lowest-order Feynman diagrams in the evaluation of the cross section and assuming a thermal mass $m_{\rm th}=gT/\sqrt{6}$, the rate of photon production in a quark-gluon plasma at temperature $T$ is [9] [Eq. (16.66) of Ref. [2]]

$$E_\gamma\frac{dN_\gamma}{d\mathbf{p}_\gamma d^4x}=\frac{5}{9}\frac{\alpha_e\alpha_s}{2\pi^2}f_q(\mathbf{p}_\gamma)T^2\ln\left\{\frac{3.7388E_\gamma}{g^2T}\right\}, \quad (55)$$

where $g^2/4\pi=\alpha_s$ is the strong-interaction coupling constant, and $f_q(\mathbf{p}_\gamma)$ is the Fermi-Dirac distribution of the quarks in the plasma which, for $E_\gamma\gg T$, is approximately the Boltzman distribution

$$f_q(\mathbf{p}_\gamma)\sim e^{-E_\gamma/T}.$$

One can introduce the $K$-factor to take into account the next-to-leading-order effect. The $K(E_\gamma)$-factor as shown in Fig. 1(a) obtained for parton collisions (at $\sqrt{s}=17.3$ GeV) can be used as an approximate $K$-factor for constituent collisions in the quark-gluon plasma. The photon distribution per event is then

$$E_\gamma\frac{dN_\gamma}{d\mathbf{p}_\gamma}=\frac{5}{9}\frac{K(E_\gamma)\alpha_e\alpha_s}{2\pi^2}\int d^4x f_q(\mathbf{p}_\gamma)T^2\ln\left\{\frac{3.7388E_\gamma}{g^2T}\right\}. \quad (56)$$

We shall assume Bjorken hydrodynamics in which the proper time varies with temperature $T$ as

$$\frac{\tau}{\tau_0}=\left(\frac{T_0}{T}\right)^3, \quad (57)$$

where $\tau_0$ is the initial proper time when the system is at a temperature $T_0$. We consider a system with an initial volume

of $V$ given by $\mathcal{A}\tau_0$ where $\mathcal{A}$ is the average overlap area for the range of impact parameters considered. Then, during the evolution of the system from temperature $T_0$ to the critical phase-transition temperature $T_c$ in the quark-gluon plasma phase, the number of photons emitted can be obtained by carrying out the integration in Eq. (56). The result is

$$E_\gamma \frac{dN_\gamma}{d\mathbf{p}_\gamma} = \frac{5K(E_\gamma)\alpha_e\alpha_s}{6\pi^2}\left(\frac{V\tau_0 T_0^4}{\hbar^4}\right)\frac{1}{T_0 E_\gamma} \times\left[E_1(z)+e^{-z}\ln\left(\frac{3.7388z}{4\pi\alpha_s}\right)\right]_{z=E_\gamma/T_c}^{z=E_\gamma/T_0}, \quad (58)$$

where $E_1(z)$ is the exponential integral $\int_z^\infty dt e^{-t}/t$ [42].

The photon distribution from the quark-gluon plasma for $T_c=200$ MeV and different values of $T_0$ is shown in Fig. 8 for the 10% most-inelastic central collisions of Pb on Pb, where we have taken the initial time parameter $\tau_0$ to be 1 fm/$c$. As one observes, the photon numbers increase as initial temperature increases. This arises because it takes a longer period of time to cool a system to the phase transition temperature if the system is initially at a higher temperature. The photon number distributions from hard scattering of partons are also shown in Fig. 8. One observes that the photon distribution from the quark-gluon plasma is greater than that from the hard scattering when the initial temperature of the plasma exceeds about 0.28 GeV.

In Fig. 9, we show the prediction for photon production when both the hard-scattering contributions and the quark-gluon plasma contributions are added together, for the 10% most-inelastic central collisions of Pb on Pb at 158 GeV per nucleon. The hard-scattering results are obtained from the LO+NLO+PT calculations. The total distribution depends on the plasma initial temperature. They have been calculated by assuming a critical temperature $T_c=200$ MeV. They may be used to compare with experimental data.

## IX. DISCUSSIONS AND CONCLUSIONS

In order to detect photons which are emitted during the quark-gluon plasma phase, it is necessary to determine the contribution of photons by non-quark-gluon plasma sources. The hard scattering between partons also produces photons in the momentum region of interest. It is therefore important to study the hard-scattering contribution to photon production in the intermediate $p_{\gamma T}$ region of a few GeV/$c$.

For photon production at $\sqrt{s}\ll 63$ GeV and $p_{\gamma T}$ up to about 6 GeV/$c$, the effects of the intrinsic transverse momenta of the partons cannot be neglected. We have examined how the intrinsic transverse momentum distribution of partons affects the transverse momentum distribution of the photons produced in nucleon-nucleon collisions. The intrinsic momentum of the partons leads to an enhancement of the cross section by a factor ranging from 3 to 8 for photons with intermediate $p_{\gamma T}$. Such an effect is an important consideration in photon measurements under investigation in high-energy heavy-ion collisions.

We have also compared the magnitude of photons produced by hard scattering with photons produced by the quark-gluon plasma. We find that for photon production in the region of 1–3 GeV/$c$ in Pb-Pb central collisions at 158 GeV per nucleon the quark-gluon plasma contribution exceeds the hard-scattering contribution when the initial temperature is greater than about 0.28 GeV.

## ACKNOWLEDGMENTS

One of us (H.W.) would like to thank Dr. G. R. Young and Dr. M. R. Strayer for their hospitality at ORNL. The authors would like to thank Professor P. Aurenche and Professor J. F. Owens for their kind help to provide the programs for the next-to-leading-order calculations. The authors would like to thank Dr. T. C. Awes for helpful discussions. This research was supported by the Division of Nuclear Physics, U.S. D.O.E. under Contract No. DE-AC05-96OR22464 managed by Lockheed Martin Energy Research Corp.

[1] Proceedings of the Quark Matter '96 Conference, Heidelberg, 1996, edited by P. Braun-Munzinger, H. J. Specht, R. Stock, and H. Stöcker [Nucl. Phys. **A610** (1996)].
[2] C. Y. Wong, *Introduction to High-Energy Heavy-Ion Collisions* (World Scientific, Singapore, 1994).
[3] R. C. Hwa, *Quark-Gluon Plasma* (World Scientific, Singapore, 1995), Vol. 2.
[4] J. Stachel and G. R. Young, Annu. Rev. Nucl. Part. Sci. **42**, 537 (1992).
[5] J. W. Harris and B. Müller, Annu. Rev. Nucl. Part. Sci. **46**, 71 (1996).
[6] R. C. Hwa and K. Kajantie, Phys. Rev. D **32**, 1109 (1985).
[7] L. D. McLerran and T. Toimela, Phys. Rev. D **31**, 545 (1985).
[8] K. Kajantie, J. Kapusta, L. McLerran, and A. Mekjian, Phys. Rev. D **34**, 2746 (1986).
[9] J. Kapusta, P. Lichard, and D. Seibert, Phys. Rev. D **44**, 2774 (1991); **47**, 4171(E) (1993); R. Baier, H. Nakkagawa, A. Niegawa, and K. Redlich, *ibid.* **45**, 4323 (1992); Z. Phys. C **53**, 433 (1992).
[10] D. K. Srivastava, B. Sinha, M. Gyulassy, and X. N. Wang, Phys. Lett. B **276**, 285 (1992).
[11] R. Albrecht *et al.*, WA80 Collaboration, Phys. Rev. Lett. **76**, 3506 (1996).
[12] T. Peitzmann *et al.*, WA98 Collaboration, Nucl. Phys. **A610**, 200c (1996).
[13] B. Wyslouch *et al.*, WA98 Collaboration, Proceedings of Quark Matter '98, Japan, 1998.
[14] L. Xiong, E. V. Shuryak, and G. E. Brown, Phys. Rev. D **46**, 3798 (1992).
[15] C. M. Hung and E. V. Shuryak, hep-ph/9608299.
[16] J. V. Steele, H. Yamagishi, and I. Zahed, Phys. Lett. B **384**, 255 (1996); hep-ph/9704414.
[17] G. Q. Li and G. E. Brown, nucl-th/9706076.
[18] P. Aurenche, R. Baier, A. Douiri, M. Fontannaz, and D. Schiff, Nucl. Phys. **B286**, 553 (1987).

[19] P. Aurenche, R. Baier, A. Douiri, M. Fontannaz, and D. Schiff, Nucl. Phys. **B297**, 261 (1988).
[20] H. Baer, J. Ohnemus, and J. F. Owens, Phys. Rev. D **42**, 61 (1990).
[21] J. Cleymans, E. Quack, K. Redlich, and D. K. Srivastava, Int. J. Mod. Phys. A **20**, 2941 (1995).
[22] J. F. Owens, Rev. Mod. Phys. **59**, 465 (1987).
[23] L. Apanasevich *et al.*, E706 Collaboration, hep-ex/9711017.
[24] L. Zielinski, in Proceedings of High-Energy Physics Conference, Dallas, 1992, Vol. 1, p. 819.
[25] X. F. Guo and J. W. Qiu, Phys. Rev. D **53**, 6144 (1996).
[26] D. W. Duke and J. F. Owens, Phys. Rev. D **30**, 49 (1984).
[27] G. Sterman *et al.*, CTEQ Collaboration, Rev. Mod. Phys. **67**, 157 (1995).
[28] H. L. Lai *et al.*, CTEQ Collaboration, Phys. Rev. D **51**, 4763 (1995); H. L. Lai, J. Huston, S. Kuhlmann, F. Olness, J. Owens, D. Soper, W. K. Tung, and H. Weerts, *ibid*. **55**, 1280 (1997).
[29] A. D. Martin, R. G. Roberts, and W. J. Stirling, Phys. Lett. B **387**, 419 (1996).
[30] R. Blankenbecler and S. J. Brodsky, Phys. Rev. D **10**, 2973 (1974).
[31] D. Sivers, S. J. Brodsky, and R. Blankenbecler, Phys. Rep., Phys. Lett. **23C**, 1 (1976).
[32] R. D. Field, *Applications of Perturbative QCD* (Addison-Wesley, Reading, MA, 1989).
[33] L. Chatterjee and C. Y. Wong, Phys. Rev. C **51**, 2125 (1995).
[34] C. Y. Wong and L. Chatterjee, Heavy Ion Phys. **4**, 201 (1996).
[35] C. Y. Wong and L. Chatterjee, Z. Phys. C **75**, 523 (1997).
[36] D. M. Kaplan *et al.*, Phys. Rev. Lett. **40**, 435 (1978).
[37] D. L. Adams *et al.*, E704 Collaboration, Phys. Lett. B **345**, 569 (1995).
[38] M. McLaughlin *et al.*, E629 Collaboration, Phys. Rev. Lett. **31**, 971 (1983).
[39] J. Badier *et al.*, Z. Phys. C **31**, 341 (1986).
[40] E. Anassonatzis *et al.*, R806/807 Collaboration, Z. Phys. C **13**, 277 (1982).
[41] A. L. S. Angelis *et al.*, R108 (CCOR) Collaboration, Phys. Lett. **94B**, 106 (1980).
[42] M. Abramowitz and I. Stegun, *Handbook of Mathematical Functions* (Dover Publications, New York, 1965), p. 227.